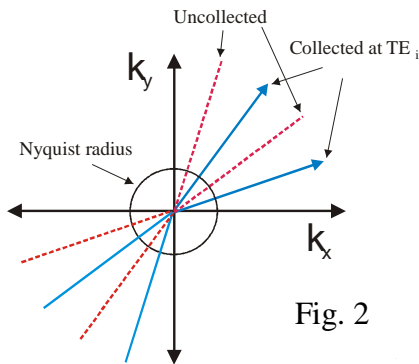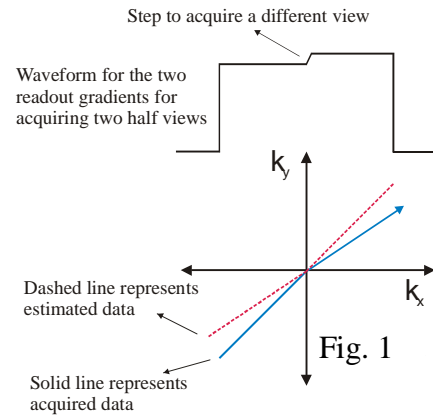# A Half Fourier Radial Fast Spin-Echo Method Using a Bent Radial Trajectory

A. Bilgin[1], A. F. Gmitro[2,3], W. F. Block[4], M. I. Altbach[2]

[1]Dept. of Electrical and Computer Eng., University of Arizona, Tucson, AZ, United States, [2]Department of Radiology, University of Arizona, Tucson, AZ, United States, [3]Optical Sciences Center, University of Arizona, Tucson, AZ, United States, [4]Biomedical Engineering and Medical Physics, University of Wisconsin-Madison, Madison, WI, United States

Introduction: Radial k-space acquisitions have been proposed as an alternative to rectilinear k-space acquisitions because they offer a number of advantages. The use of radial acquisitions has been shown to yield significant motion artifact reduction[1]. Furthermore, the inherent oversampling of the low spatial frequencies in radial trajectories has been exploited to manipulate contrast[2-4]. In particular, radial fast spin-echo (RAD-FSE)[2,3] or radial gradient and spin-echo (RAD-GRASE)[4] methods have been used to obtain high-resolution images at various effective TEs from a single k-space data set. These images were then used to calculate T2 (or T2*) maps for tissue characterization. The RAD-FSE and RAD-GRASE methods are based on acquiring full radial views. It is possible to improve the time efficiency of these methods, if partial Fourier acquisition and reconstruction methods are used[5-9]. In this work, we propose a "bent" RAD-FSE pulse sequence that allows the creation of two radial views in the time required for acquisition of one full radial view. Previously, this acquisition strategy has been applied to 3D projection imaging[8].

Step to acquire a different view

Waveform for the two readout gradients for acquiring two half views

Dashed line represents estimated data

Solid line represents acquired data

Fig. 1

Uncollected

Collected at TE$_i$

Nyquist radius

Fig. 2

Method: The "bent" k-space trajectory and the corresponding readout gradient are illustrated in Fig. 1. As shown in the figure, the gradient amplitude is modified at the center of k-space to change the angle of the projection. The solid lines in the figure represent the acquired data, and the dashed lines represent the uncollected data. The uncollected half of each radial view is estimated using the single-TE interpolation method[9]. In this method, the uncollected k-space points that are within the Nyquist radius are calculated using linear interpolation. The optimal angular view ordering in RAD-FSE requires the neighboring views to be collected at different TEs[10]. However, mixing of neighboring views collected with different signal weighting results in smearing. In order to avoid this smearing, only views that are collected at a specific TE are used during interpolation. This is illustrated in Fig. 2. Note that the Nyquist radius is calculated based on the k-space sampling between views at a single TE. The uncollected k-space points outside the Nyquist radius are calculated using homodyne detection in the projection domain[6]. Let $F(\theta, w)$ denote the k-space data in polar coordinates and $P_\theta(t) = |P_\theta(t)|e^{i\phi(t)} = F^{-1}\{F(\theta, w)\}$ the projection at angle θ. Then, the projection obtained using the half k-space data at angle θ is given by $P_\theta^{half}(t) = F^{-1}\{F(\theta, w)u(w)\}$, where $u(w)$ is the unit step function. The relation between $P_\theta(t)$ and $P_\theta^{half}(t)$ can be written in the projection domain as $P_\theta^{half}(t) = \frac{1}{2}|P_\theta(t)|e^{i\phi(t)} + i\frac{1}{2}\left[|P_\theta(t)|e^{i\phi(t)} * \frac{1}{\pi t}\right]$. If we assume that the phase of the projection $\phi(t)$ is slowly varying, and $\hat{\phi}(t)$ is an estimate of this phase, this equation can be rearranged to give $P_\theta^{half}(t) \approx |P_\theta(t)|e^{i\hat{\phi}(t)} \approx 2\left[P_\theta^{half}(t)e^{-i\hat{\phi}(t)}\right]e^{i\hat{\phi}(t)}$. This equation is used to approximate $P_\theta(t)$ using $P_\theta^{half}(t)$ and the phase estimate $\hat{\phi}(t)$ which is computed using only the k-space points within the Nyquist radius at the specified TE. Once the projections $P_\theta(t)$ are calculated for all θ, the image can be reconstructed using either back-projection or regridding. It is worth reiterating that the phase correction in this method is performed in the projection domain under the assumption that the phase of each projection is slowly varying. This projection domain correction yielded satisfactory results with the radial fast spin-echo data.

Results and Discussion: The bent RAD-FSE technique was implemented on a 1.5 T MRI GE Signa scanner equipped with a 40 mT/m shielded gradients. To evaluate the method, we compare the images obtained using bent RAD-FSE to images obtained using a full-view RAD-FSE pulse sequence. In both cases, data were acquired with an ETL=8, read out points=256, echo spacing of 8.8 ms, and receiver bandwidth of ±31.2 kHz. Figs. 3a and 3b show the images reconstructed using the full k-space data set with 160 and 80 (full) views, respectively. Fig. 3c shows the image obtained using the bent k-space trajectory with 80 bent views and single-TE interpolation method. The images on Figs. 3b and 3c are acquired in half the time compared to the image on Fig. 3a. However, if data is acquired with 80 (full) views, there are significant streaking artifacts due to undersampling. These are greatly reduced if the bent RAD-FSE method is used.
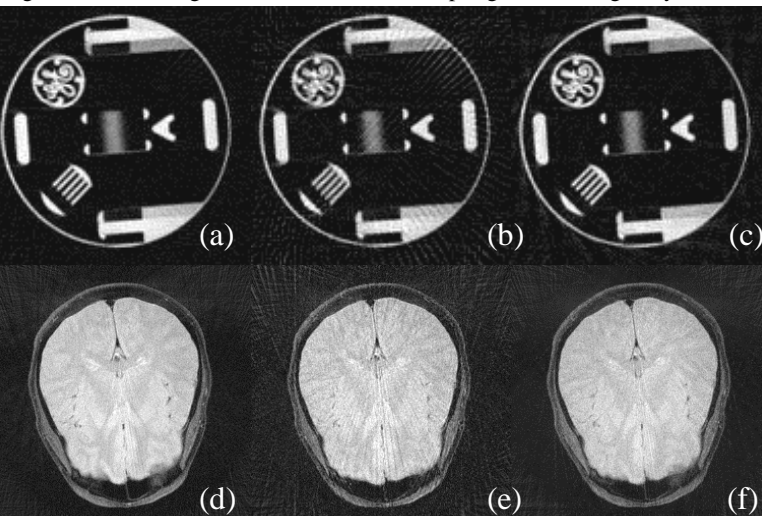

In vivo examples are presented in Figs. 3d-3f. Figs. 3d and 3e show the images reconstructed using the full k-space data set with 128 and 64 (full) views, respectively. Fig. 3f shows the image obtained with 64 bent views. In this case as well, the streaking artifacts due to undersampling are significantly reduced in the image obtained with bent RAD-FSE.

Conclusion: A RAD-FSE pulse sequence that reduces the undersampling artifacts by allowing the generation of twice the number of views in the same scan time is presented. The technique can either be used to reduce the scan time or the undersampling artifact level. A similar sequence can be developed for other radial methods such as RAD-GRASE[4].

References: [1] Glover GH, MRM 28, 275 (1992) [2] Song HK, MRM, 44, 825 (2000). [3] Altbach MI, JMRI, 16, 179 (2002). [4] Gmitro AF, Proc. ISMRM, 2003. [5] Noll DC, IEEE TMI, 10, 154 (1991). [6] Noll DC, Proc. SPIE, 1443, 29 (1991). [7] Block WF, Proc. ISMRM, (1999). [8] Toropov, Proc. ISMRM (2001). [9] Bilgin A, Proc. ISMRM, (2004). [10] Theilmann BJ, MRM, 51, 768 (2004).

Fig. 3. Images reconstructed from: (a) 160 full views, (b) 80 full views, (c) 80 bent views, (d) 128 full views, (e) 64 full views, (f) 64 bent views.